Nitrogen-induced enhancement of the electron effective mass in InN_xAs_{1-x}

W. K. Hung, K. S. Cho, M. Y. Chern, and Y. F. Chen[a]
Department of Physics, National Taiwan University, Taipei, Taiwan, Republic of China

D. K. Shih and H. H. Lin
Department of Electrical Engineering, National Taiwan University, Taipei, Taiwan, Republic of China

C. C. Lu and T. R. Yang
Department of Physics, National Taiwan Normal University, Taipei, Taiwan, Republic of China

(Received 6 September 2001; accepted for publication 14 November 2001)

The electron effective mass in n-type InN_xAs_{1-x} (with x up to 3.0%) grown by gas-source molecular-beam epitaxy was obtained from infrared reflectivity and Hall-effect measurements. The large increase of the effective mass due to the incorporation of nitrogen is attributed mainly to the nitrogen-induced modification on the electronic states near the conduction-band edge. The well-known band anticrossing (BAC) model for the electronic structure of the III-N-V alloys cannot well describe the experimental data, especially in the region of higher electron concentration. This result provides an opportunity to examine the "universality" of the BAC model. © *2002 American Institute of Physics.* [DOI: 10.1063/1.1436524]

III-N-V alloys such as Ga(In)NAs, GaNP, and InNP have been found to exhibit particular physical properties and potential applications in long-wavelength optoelectronic devices.[1–6] The incorporation of nitrogen into the host III–V crystal causes a significant reduction (giant bowing) in the fundamental band gap,[4,5] reduced temperature and pressure dependence of the band-gap energy,[7,8] and a large increase in the electron effective mass.[9–11] These unusual behaviors are usually explained in terms of the band anticrossing (BAC) model in which the localized N resonant states interact with the extended conduction-band (CB) states, leading to the splitting of the CB into two nonparabolic subbands.[7] Alternatively, the theoretical calculations based on the pseudopotential local density approximation indicates that the N-induced mixing between the Γ and L states is responsible for these phenomena.[12]

InN_xAs_{1-x} should be a promising material for infrared technology since InAs has a narrow band gap of 0.36 eV at room temperature. Up to now, there were only very limited efforts directed to this alloy.[13–15] Naoi, Naoi, and Sakai grew InNAs films on GaAs substrates by metalorganic chemical-vapor deposition and found the band gap reduced to 0.12 eV with nitrogen composition up to 6%.[13] However, except for a photoluminescence study on $InN_xAs_{1-x}/InGa_xAs_{1-x}$ single quantum wells,[15] no further experimental studies on the electronic properties of InNAs were reported. Knowledge of the carrier effective mass provides valuable information on the fundamental nature of the band states in the alloy and is also important for a full exploration and optimization of this material system in device applications. In this work, we report measurements of the electron effective mass in InN_xAs_{1-x} with various N contents and electron concentrations. The effective mass is greatly enhanced due to the N incorporation. However, in contrast to the case of Ga(In)NAs, we find that the simple BAC model may be not suitable to describe the effective mass in the InNAs alloy systems.

The InNAs films were grown on semi-insulating (001) InP substrates using a VG V-80 gas-source molecular-beam epitaxy system. An element In source and thermally cracked AsH_3 were used for producing molecular beams. The active N species were generated from an EPI UNI-bulb rf plasma source. The growth temperature for InNAs was 460 °C. Details of the growth conditions are reported elsewhere.[16] The films are about 2.5 μm thick and intentionally undoped. The samples were examined with a high-resolution x-ray diffractometer using the Cu $K\alpha_1$ line (with wavelength 1.54 Å). The N compositions were determined by assuming that the InNAs films are fully relaxed and Vegard's law holds. The former assumption is justified by the fact that the film thickness is much larger than the critical thickness calculated from the Matthews and Blakeslee model.[17] The lattice constants of InP, InAs, and cubic InN are taken to be 5.8688, 6.0584, and 4.98 Å, respectively. The electrical properties were investigated by Hall-effect measurements in the Van der Pauw configuration. The results are summarized in Table I. The samples containing nitrogen are intrinsically n type and the electron concentration increases with the incorporated N concentration. The possible origin of the high carrier concentration in these samples is not yet clear.

The infrared reflectivity measurements were performed

TABLE I. Parameters of the studied samples. All measurements were performed at room temperature.

Sample number	N(%)	Thickness (nm)	n (cm^{-3})	Mobility (cm^2 V^{-1} s^{-1})	m^*/m_0 (experiment)
A	0	⋯	2.64×10^{16}	7660	0.024
B	0.2	2465	1.91×10^{18}	1740	0.063
C	2.2	2670	2.80×10^{18}	1010	0.058
D	2.4	2460	3.24×10^{18}	1280	0.068
E	3.0	2580	1.69×10^{19}	38	0.326

[a]Electronic mail: yfchen@phys.ntu.edu.tw

 © 2002 American Institute of Physics

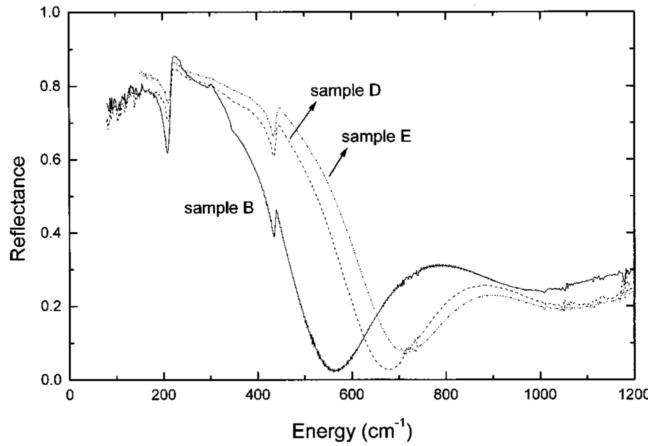

FIG. 1. (a) Reflectivity spectra for three InN_xAs_{1-x} samples.

at room temperature with a Bruker IFS 120 HR Fourier transform infrared spectrometer. Figure 1(a) shows the reflectivity spectra of three InN_xAs_{1-x} samples. The features at about 307.2 and 347.5 cm^{-1} correspond to InP transverse optical (TO) and longitudinal optical (LO) phonons, respectively. We attribute the peak at about 225 cm^{-1} to the InAs-like TO mode, and the peak at about 440 cm^{-1} to the InN-like TO mode. The plasma reflection edge is evidently observed and shifts to higher energy with increasing electron concentration.

Electron effective mass m^* is obtained by fitting the reflectivity spectra with a three-layer structure (air–InNAs–InP) model. The dielectric function of InP is taken from the literature. Dielectric function ϵ of InNAs can be modeled with an additive form[18]

$$\epsilon=\epsilon_\infty+\sum_{j=1}^{2}\frac{S_j}{\omega_{Tj}^2-\omega^2-i\Gamma_j\omega}-\frac{\epsilon_\infty\omega_p^2}{\omega(\omega+i\gamma)}, \tag{1}$$

where ϵ_∞ is the high-frequency dielectric constant (taken to be 12.25, the same as InAs); ω_{Tj}, Γ_j, and S_j are the resonance frequency, damping constant, and strength of the jth TO mode (InAs and InN-like), respectively. The last term in Eq. (1) represents the free-carrier contribution with frequency-independent damping constant γ and plasma frequency ω_p. The electron effective mass at the Fermi energy can be determined from[18,19]

$$m^*=\frac{4\pi ne^2}{\epsilon_\infty\omega_p^2}, \tag{2}$$

where e is the electron charge, and n is the electron concentration. The obtained values of the film thickness and effective mass are also listed in Table I. We see that the effective mass increases largely as nitrogen atoms are introduced into the InAs host.

The experimental effective mass obtained above is plotted against the electron concentration in Fig. 2. It is well known that due to the CB nonparabolicity the electron effective mass in heavily doped narrow-band-gap semiconductors strongly depends on the electron concentration. To evaluate this effect, we use the simple two-band Kane model[20,21] to calculate the InAs effective mass m_M at the electron concentration of our samples. The momentum matrix element P^2 in the Kane model is taken to be 11.9 eV, as in Ref. 20, and the results are consistent with the values found in the literature.[20] The calculated m_M, also plotted in Fig. 2, is too small to account for the experimental data. Thus, it is clear that the enhancement of the effective mass should be mainly due to the N-induced modification of the CB structure.

The BAC model is known to predict a large increase of the electron effective mass.[10,22] In the model, the interaction of N states with the extended states of the semiconductor matrix results in the formation of two conduction subbands E_- and E_+ given by[7]

$$E_\pm(k)=\tfrac{1}{2}\{[E_M(k)+E_N]\pm\sqrt{[E_M(k)-E_N]^2+4C_{NM}^2x}\}, \tag{3}$$

where E_N is the energy of the N state, $E_M(k)$ is the dispersion relation for the CB of the host crystal, and C_{NM} is the matrix element describing the coupling between these two types of states. All the energies are relative to the top of the valence band. Due to its localized nature, the energy E_N of the N level can be estimated to be 1.48 eV from valence-band offset Δ (GaAs/InAs) = 0.17 eV and from E_N

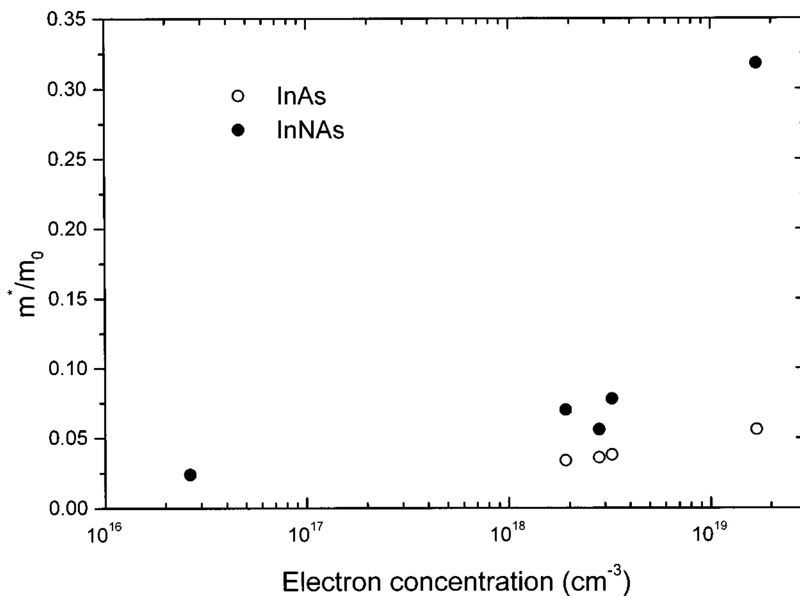

FIG. 2. Effective mass vs electron concentration n. Closed circles denote the experimental data for InN_xAs_{1-x}, while open circles denote the calculated effective mass for InAs.

$=1.65$ eV in GaAs.[7,23] C_{NM} is taken as 1.92 eV to fit the band-gap energy measured by Naoi, Naoi, and Sakai.[13] It should be noted that in the simple BAC model only the anticrossing interaction between the extended states of the Γ CB and the localized N level is considered. The interaction between L (or X) and the N level is neglected due to the symmetry selection rules.[24]

From Eq. (3) an analytic expression for the k dependence of the inverse effective mass can be written as (considering only the E_- branch)[10]

$$\frac{1}{m^*(k)} = \frac{1}{2m_M(k)}\left\{1 - \frac{[E_M(k)-E_{\rm N}]}{\sqrt{[E_M(k)-E_{\rm N}]^2+4C_{NM}^2 x}}\right\}, \tag{4}$$

where energy-dependent $m_M(k)$ and $E_M(k)$ are calculated by the two-band Kane model, as mentioned above. The effective mass is calculated at the Fermi surface, i.e., at $k=k_F=(3\pi^2 n)^{1/3}$. One notes that due to the relatively large energy difference between $E_{\rm N}$ and E_M $[E_{\rm N}-E_M(k_F)\sim 1$ eV, here], the composition-dependent term $C_{NM}^2 x$ has little effect on the effective mass. That is, m^* should approximately approach m_M for InAs. Furthermore, one should note that effective mass $m^*(k)$ calculated from Eq. (4) never exceeds $2m_M(k)$ if $E_M(k)<E_N$. However, as shown in Fig. 2, the measured effective mass either approaches $2m_M$, which corresponds to extremely large C_{NM}, or exceeds 2 m_M (especially for the sample with the highest electron concentration). Thus, the simple BAC model fails to describe the experimental data.

According to our experimental results, it seems more plausible to view the CB edge of InN_xAs_{1-x} as a mixing state which has components of the Γ, L, and X states of InAs. Such a mixing is caused by the strong perturbation introduced by substitution of N on an As site.[12] As illustrated in the case of GaN_xAs_{1-x}, the CB edge shows a reduced (increased) $\Gamma(L)$ character as x increases (for x approaches 0.8%, the L component approaches 12%).[12] Since the L electrons have much heavier mass than the Γ [for InAs, $m_t(L)\sim 0.05$, $m_l(L)\sim 0.64$], effective mass $m^*(k_F)$ has the possibility to exceed $2m_M$.

In summary, the effective mass of InN_xAs_{1-x} with different N compositions and electron concentrations was obtained from infrared reflectivity and Hall-effect measurements. We point out that the large increase of the effective mass is probably due to the N-induced modification on the electronic structure near the conduction-band edge. Our results, therefore, calls for further theoretical efforts in order to clarify the role of the nitrogen state in the perturbation of the band structure.

This work was supported by the National Science Council and Ministry of Education of the Republic of China.

[1] I. A. Buyanova, W. M. Chen, and B. Monemar, MRS Internet J. Nitride Semicond. Res. **6**, 1 (2001).
[2] M. Kondow, K. Uomi, T. Kitatani, S. Watahiki, and Y. Yazawa, J. Cryst. Growth **164**, 175 (1996).
[3] G. S. Kinsey, D. W. Gotthold, A. L. Holmes, Jr., B. G. Streetman, and J. C. Campbell, Appl. Phys. Lett. **76**, 2824 (2000).
[4] J. F. Geisz, D. J. Friedman, J. M. Olson, S. R. Kurtz, and B. M. Keyes, J. Cryst. Growth **195**, 401 (1998).
[5] M. Weyers, M. Sato, and H. Ando, Jpn. J. Appl. Phys., Part 2 **31**, L853 (1992).
[6] K. M. Yu, W. Walukiewicz, J. Wu, J. W. Beeman, J. W. Ager III, E. E. Haller, W. Shan, H. P. Xin, and C. W. Tu, Appl. Phys. Lett. **78**, 1077 (2001).
[7] W. Shan, W. Walukiewicz, J. W. Ager III, E. E. Haller, J. F. Geisz, D. J. Friedman, J. M. Olson, and S. R. Kurtz, Phys. Rev. Lett. **82**, 1221 (1999).
[8] I. Suemune, K. Uesugi, and W. Walukiewicz, Appl. Phys. Lett. **77**, 3021 (2000).
[9] P. N. Hai, W. M. Chen, I. A. Buyanova, H. P. Xin, and C. W. Tu, Appl. Phys. Lett. **77**, 1843 (2000).
[10] C. Skierbiszewski, P. Perlin, Pl Wisniewski, W. Knap, T. Suski, W. Walukiewicz, W. Shan, K. M. Yu, J. W. Ager III, E. E. Haller, J. F. Geisz, and J. M. Olson, Appl. Phys. Lett. **76**, 2409 (2000).
[11] Z. Pan, L. H. Li, Y. W. Lin, B. Q. Sun, D. S. Jiang, and W. K. Ge, Appl. Phys. Lett. **78**, 2217 (2001).
[12] T. Mattila, S.-H. Wei, and A. Zunger, Phys. Rev. B **60**, R11245 (1999).
[13] H. Naoi, Y. Naoi, and S. Sakai, Solid-State Electron. **41**, 319 (1997).
[14] R. Beresford, K. S. Stevens, and A. F. Schwartzman, J. Vac. Sci. Technol. B **16**, 1293 (1998).
[15] J. C. Fan, W. K. Hung, Y. F. Chen, J. S. Wang, and H. H. Lin, Phys. Rev. B **62**, 10990 (2000).
[16] D. K. Shih, H. H. Lin, L. W. Song, T. Y. Chu, and T. R. Yang, Proceedings International Conference of the 13th on Indium Phosphide and Related Materials, Nara, Japan, 2001 (unpublished), p. 555.
[17] J. W. Matthews and A. E. Blakeslee, J. Cryst. Growth **27**, 118 (1974).
[18] S. Perkowitz, *Optical Characterization of Semiconductors: Infrared, Raman, and Photoluminescence Spectroscopy* (Academic, London, 1993).
[19] W. Zawadzki, Adv. Phys. **23**, 435 (1974).
[20] Y. B. Li, R. A. Stradling, T. Knight, J. R. Birch, R. H. Thomas, C. C. Phillips, and I. T. Ferguson, Semicond. Sci. Technol. **8**, 101 (1992).
[21] E. O. Kane, J. Phys. Chem. Solids **1**, 249 (1957).
[22] A. Lindsay and E. P. O'Reilly, Solid State Commun. **112**, 443 (1999).
[23] D. J. Wolford, J. A. Bradley, K. Fry, and J. Thompson, in *Proceedings of the 17th International Conference on the Physics of Semiconductors*, edited by J. D. Chadi and W. A. Harrison (Springer, New York, 1984), p. 627.
[24] W. K. Hung, M. Y. Chern, Y. F. Chen, Z. L. Yang, and Y. S. Huang, Phys. Rev. B **62**, 13028 (2000).

Applied Physics Letters is copyrighted by the American Institute of Physics (AIP). Redistribution of journal material is subject to the AIP online journal license and/or AIP copyright. For more information, see http://ojps.aip.org/aplo/aplcr.jsp
Copyright of Applied Physics Letters is the property of American Institute of Physics and its content may not be copied or emailed to multiple sites or posted to a listserv without the copyright holder's express written permission. However, users may print, download, or email articles for individual use.